FEM model of the low-cycle damage at the fatigue crack tip

Aleš Materna[1, a] and Vladislav Oliva[1,b]

[1]Department of Materials, Faculty of Nuclear Sciences and Physical Engineering,
Czech Technical University in Prague,
Trojanova 13, 120 00 Praha 2, Czech Republic

[a]Ales.Materna@fjfi.cvut.cz, [b]Vladislav Oliva@fjfi.cvut.cz

Keywords: fatigue crack growth, FEM model, SWT parameter, low-cycle fatigue, blunted crack tip.

Abstract. A new 2D elastic-plastic FEM model for prediction of the fatigue crack growth is presented and compared with experimental results. The model is based on the idea of local low-cycle fatigue of a small material volume in front of the high cycle crack. A fatigue crack tip blunting and a step crack advance are modelled through a successive deactivation of elements at the crack tip. The following reactivation of the elements in a foregoing stress-strain state and implementation of a contact algorithm allow to respect an possible crack closure. The deactivation of the crack tip element and related elementary crack jump occur at a critical low-cycle damage accumulation in the element. The immediate rate of the damage accumulation is given by the product of maximum stress and elastic-plastic strain amplitude (Smith-Watson-Topper parameter) in the loading cycle. From the material point of view, only a stress-strain curve and standard low-cycle fatigue results are sufficient to simulate the fatigue crack growth. The model is able to qualitatively describe the retardation effect after application of a single overload.

Introduction

Current standard methods for predicting the fatigue life of components with cracks are mostly based on the stress intensity factor K. Alternatively, techniques based on the cumulative low-cycle damage in front of the crack tip are studied (e.g. [1]). Contrary to the pure elastic K-concept, these methods are computationally more complicated because the knowledge of cyclic stress and elastic-plastic strain fields is required. On the other hand, such models with a properly chosen damage criterion could lead to more general description of the fatigue crack growth behaviour. They should enable direct simulation of residual stresses leading to plasticity-induced crack closure and, also, they are able to take into account various strain constraint at the crack front given by various component thickness.

The authors' long-term effort has been to improve three-dimensional "low-cycle crack tip fatigue" numerical model of planar fatigue crack growth [2]. In an ideal case, such model should predict constant amplitude crack growth and take into account the stress ratio effect, component thickness, and, last but not least, variable amplitude loading.

In this contribution, basics of the proposed numerical model are presented and the potential of the model is demonstrated on a simplified plane stress simulation of the crack growth after a single overload.

Basic characterization of FEM model

Inspiration for developing the numerical model was given by an analytical model presented in [3,4]. Here, the derivation of the driving force controlling the fatigue crack growth was based on the following assumptions:

- The material is composed of elementary blocks of size ρ^*.
- The fatigue crack is regarded as a notch with the tip radius ρ^*.

- The fatigue crack growth is considered as successive crack increments due to crack re-initiations over the distance ρ^*.
- The number of cycles necessary to fail the material over the distance ρ^* is derived by using the Smith-Watson-Topper (SWT) low-cycle fatigue damage parameter [5].

The numerical model is slightly different due to discrete nature of the finite element method. The crack propagation modelling is its new key feature. An elementary crack advance is modelled by a temporary deactivation of one finite element at the crack tip, as shown in Fig. 1. The classical "node release" technique [6,7] was given up because in case of 3D simulation of planar cracks with variable crack advance along the curved front the new algorithm is easier to implement. Also, suppression of high gradients in stresses and strains induced by the unrealistically sharp crack seems to be reasonable.

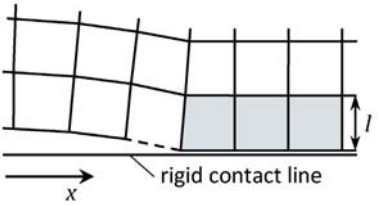

Fig. 1 – Finite element model of crack propagation. Damage accumulation is computed in gray elements.

A more detailed description of the proposed model can be summarized as follows:

1. The area in the vicinity of the whole crack growth path is covered by square linear finite elements of the size l. The value of l is characteristic for the used material model parameters (elastic constants, stress-plastic strain curve, hardening model).
2. Fatigue damage D accumulated in all elements along the crack growth path is computed and stored according to the following formulas:
   i. After each loading cycle i the maximum stress in the cycle $\sigma_{\max}(i)$ and the total strain range in the loading direction during the loading half-cycle $\Delta\varepsilon(i)$ are determined for each element. The value of SWT parameter P_{SWT}(i) is computed according to

$$P_{SWT}(i) = \sigma_{\max}(i)\frac{\Delta\varepsilon(i)}{2}. \tag{1}$$

   ii. Hypothetical life $N_f(i)$ – number of cycles to failure – of the element subjected to cyclic loading with the SWT parameter P_{SWT}(i) is determined numerically from the nonlinear equation [3]

$$P_{SWT}(i) = \frac{(\sigma'_f)^2}{E}(2N_f(i))^{2b} + \sigma'_f\varepsilon'_f(2N_f(i))^{b+c}, \tag{2}$$

   where σ'_f = fatigue strength coefficient, ε'_f = fatigue ductility coefficient, b = fatigue strength exponent, and c = fatigue ductility exponent.

   iii. Reciprocal value of $N_f(i)$ determines the damage increment in the element per the cycle i:

$$\Delta D(i) = \frac{1}{N_f(i)}. \tag{3}$$

iv. If the linear cumulative damage hypothesis is supposed, the total damage of each element is given by a simple summation of damage increments per all the previous loading cycles:

$$D = \sum_i \Delta D(i). \tag{4}$$

3. If total damage D in some element reaches the critical value 1, this finite element is temporarily deactivated; it does not contribute to the load, mass, stiffness, or internal force calculation, and it is also not present in the output results. At the moment of the next crack advance the element is reactivated with the foregoing stress and strain state. The residual strains of reactivated elements together with rigid contact algorithm (Fig. 1) can induce crack closure. The contact algorithm is used also in front of the crack tip: a commonly used kinematic boundary condition with restricted displacements in a loading direction is replaced by the contact with the very high separation force excluding the creation of the flaw. As can be seen in Fig. 1, edges of the rectangular element form a simplified model of the crack tip „blunting".
4. The actual crack length a is determined by the location of the deactivated element. Crack growth rate da/dN is given by the numerical derivation of the crack growth curve $a - N$.

Verification of the numerical model

Input material data. Material properties used in the proposed model have to reflect strain response to external cyclic stresses and the rate of fatigue damage accumulation. Therefore, the input data are obtained from common low-cycle fatigue tests. Only data of aluminium alloy 2024-T3 Clad were used for the validation of the model.

The model $\sigma - \varepsilon_p$ curve (Fig. 2) was obtained from the cyclic stress-strain curve.

The material fatigue life curve formulated in terms of SWT parameter according to Eq. 2. is shown in Fig. 3.

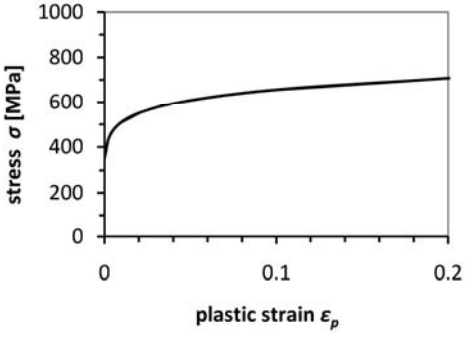

Fig. 2 – The model $\sigma - \varepsilon_p$ curve for Al 2024-T3 Clad

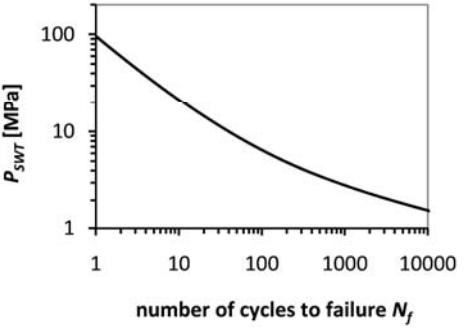

Fig. 3 – The fatigue life curve SWT parameter vs. N_f for Al 2024-T3 Clad

Fatigue crack growth experiments. The fatigue crack growth data were obtained experimentally on thin single-edge-notched specimens from 2024-T3 Clad alloy [8]. The specimen size was 200(h)×40(w)×2(t) mm, the length of the edge notch beeing 7.5 mm. A total of three specimens marked as Exp1, Exp2 and Exp3 was loaded at a stress ratio of R = 0.05. A single overload cycle

with the overload ratio $\sigma_{maxOL}/\sigma_{max}$ = 1.5 was applied to each specimen at two crack lengths a_{OL} (see Table 1). All the tests were performed on air at room temperature. The crack length was measured by an electrical potential method.

Experiment	Const. amplitude loading		Overload			
	$\Delta\sigma$ [MPa]	R	OL	a_{OL} [mm]	ΔK_{OL} [MPa m$^{1/2}$]	$\sigma_{maxOL}/\sigma_{max}$
Exp1	60	0.05	1st	11.73	14.59	1.5
			2nd	19.77	21.70	1.5
Exp2	60	0.05	1st	11.33	14.26	1.5
			2nd	17.68	19.69	1.5
Exp3	60	0.05	1st	12.02	14.83	1.5
			2nd	17.59	19.61	1.5

Table 1 – Loading of three specimens subjected to overloads [8]

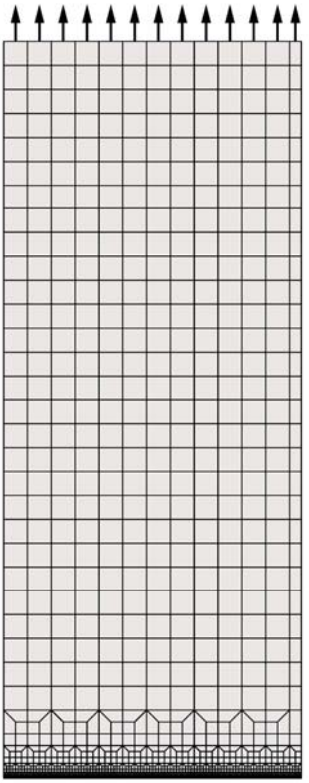

a) The FEM model

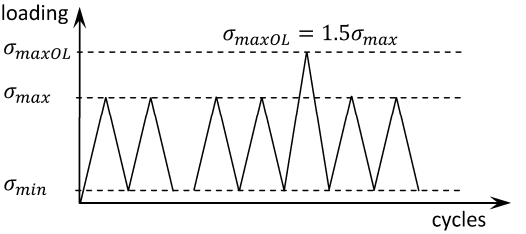

b) Cyclic loading

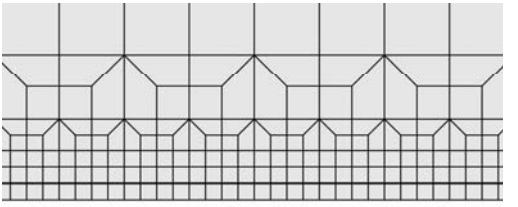

c) Detail of the mesh along the crack growth path

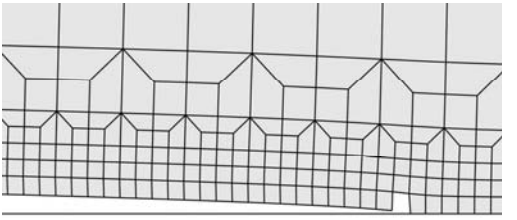

d) Detail of the deformed mesh with the deactivated element at the crack tip

Fig. 4 – Finite element mesh covers the quarter of the test specimen. Refined elements of the length l are located along the crack growth path

Finite element mesh and model. The finite element model of the growing fatigue crack was built in MSC.Marc. Fatigue damage evaluation, changing boundary conditions and all other non-standard procedures were implemented using user subroutines [9]. The specimens were modelled as two-dimensional (plane stress) bodies using linear quadrilateral elements. Due to the symmetry, only one quarter of the whole geometry was covered by the finite element mesh. The typical mesh with refined square elements along the whole crack growth path is shown in Fig. 4. Elastic-plastic computations with the small deformation formulation and isotropic hardening rule were carried out.

Estimation of the element size *l*. Authors of [3] suppose that some fatigue crack growth data are necessary to determine the elementary material block size ρ^*. Both the near threshold data at high stress ratios $R > 0.5$ and crack growth data at any stress ratio can be used.

In our model, the size l of the smallest elements plays a similar role. However, one can expect the value of l different from ρ^*. The reason lies in different modelling of the crack tip blunting, which induces different stress and strain gradients. Also, the discrete nature of finite element computation leads to the stress and strain distribution, which is different from an analytical solution. Nevertheless, the method for the element size l estimation is exactly the same: iterative procedure when l is varied and computational crack rate are compared to experimental rate.

For the case under study, three various element sizes were chosen: $l = 25$ μm, 50 μm and 100 μm. Roughly tens of thousands cycles were applied in each simulation with the length of the crack growth approximately 15 mm. Corresponding model crack growth rates are shown in Fig. 5 together with the experimental curve. Only experimental crack rates unaffected by the overload were used from Exp1 – Exp3 and fitted according to Paris law

$$\frac{da}{dN} = C(\Delta K)^m. \tag{5}$$

As can be seen in Fig. 5, the numerically predicted crack rates increase with decreasing element size. An important finding is that the slope (characterized by the exponent $m = 4.5$ in Eq. 5) of the curves estimated numerically is approximately the same as that measured experimentally. Therefore, the experimental and numerical data for the whole "Paris regime" crack growth can be correlated. The best agreement with the experiment is achieved with the element size $l = 50$ μm.

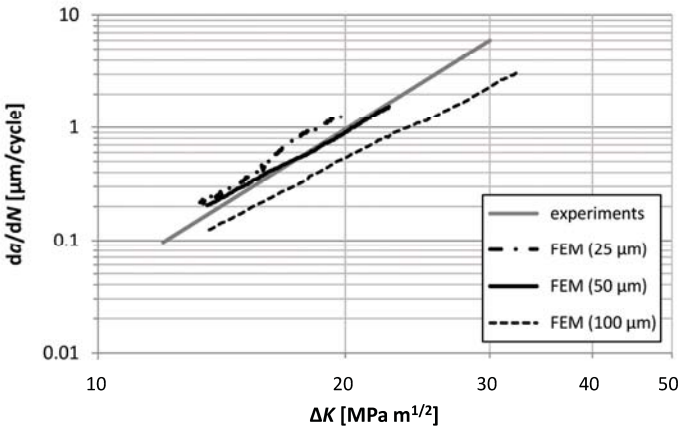

Fig. 5 – Experimental and FEM fatigue growth rates for Al 2024-T3 Clad. The best agreement is achieved with the element size of 50 μm.

Prediction of the fatigue crack growth after a single overload. The capability of the proposed model to estimate temporary retardation of the crack growth after a single overload was tested on two simulations of experiments Exp2–Exp3 described above. The first simulation included the 50% overload at the crack length $a = 11.9$ mm, the second at $a = 17.5$ mm. Both simulations use the same mesh with the smallest element size $l = 50$ μm. Model results are compared with experiments in Fig. 6 and Fig. 7.

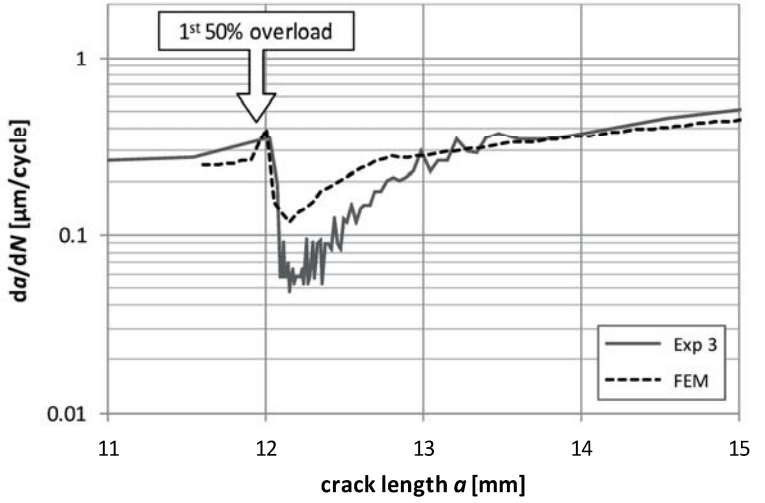

Fig. 6 – Experimental and predicted fatigue crack growth rates after 1st 50% overload (Al 2024-T3 Clad, $\Delta K = 15$ MPa $m^{1/2}$)

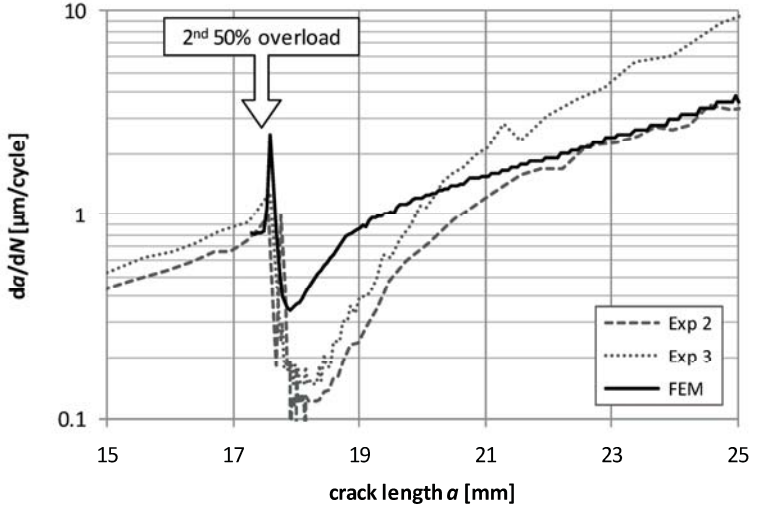

Fig. 7 – Experimental and predicted fatigue crack growth rates after 2nd 50% overload (Al 2024-T3 Clad, $\Delta K = 20$ MPa $m^{1/2}$)

The numerical results predict the well known effect of the single overload: after immediate acceleration, delayed retardation occurs for a relatively long time. Quantitatively, the overload effect can be described by the length of influenced region and by the maximum retardation parameter defined as a ratio of the minimum rate after the overload to the rate immediately before the overload. All quantities are summarized in Table 2.

source of data	crack length at OL [mm]	length of infl. region [mm]	minimum rate after OL [μm/cycle]	rate before OL [μm/cycle]	maximum retardation
Exp3	12.0	1.3	0.06	0.27	0.22
FEM	11.9	0.8	0.12	0.26	0.46
Exp2	17.7	4.0	0.12	0.86	0.14
Exp3	17.6	3.8	0.15	0.94	0.16
FEM	17.5	2.5	0.34	0.83	0.41

Table 2 – Crack growth retardation after single 50% overload in Al 2024-T3 Clad

Experimental and numerical data in Table 2 confirm that the overload effect is more intensive for the longer crack, where larger plastic zone is formed – the influenced crack path is longer and maximum retardation parameter is lower. It can also be concluded that the computational overload effect is approximately two times underestimated in comparison with real retardation for both crack lengths. With the set of results for only one material it is difficult to find a reason for a certain discrepancy between the theoretical and experimental curves. Some shortcomings of the model, which could explain the underestimation of the retardation, are as follows:

1. only plasticity-induced crack closure was modelled; roughness or other sources of closure were not involved;
2. the simplified model of crack tip blunting; "blunting" is almost independent of the stress level around the crack tip resulting from the changing crack length and external load;
3. the non-optimal model of cyclic plasticity; kinematic hardening rule should be involved to account for Bauschinger effect;
4. linear accumulation of the fatigue damage is used; real fatigue accumulation is influenced by many factors, namely load dependence, nonlinear damage evolution, load sequence effect and so on [10].

In view of the nature of the model, only points 3 and 4 could be modified. In the future simulations, attention should be paid to improved modelling of the cyclic plasticity of the material, to the potential enhancement of the damage accumulation hypothesis, and to the verification of the model on another types of materials.

Conclusions

A numerical model of the fatigue crack propagation based on the temporary deactivation of the finite element at the crack tip has been proposed. The element is deactivated at the moment its low-cycle fatigue life is exhausted. The damage of the elements along the crack growth path is determined by the linear damage rule and Smith-Watson-Topper parameter. The damage results directly from the local elastic-plastic stress-strain history and common low-cycle fatigue data for material of the cracked body. A uniform size of the elements along the crack path has to be determined from fatigue crack growth data for each new material. The comparison of the numerical and experimental data for Al alloy 2024-T3 Clad has shown that the fatigue crack growth model is able to qualitatively describe the retardation effect after a single overload, although it predicts lower

drop in crack rate. The main advantage of the model is in its universality which will allow a simple generalization to the three-dimensional cases with planar cracks. Effects of various strain constraints on local crack rates and on resulting crack front shape could be qualitatively studied.

Acknowledgement

Research support from the Czech Science Foundation No. GA101/08/1623 is acknowledged.

References

[1] R. P. Skelton, T. Vilhelmsen and G. A. Webster: Int. J. Fatigue Vol. 20 (1998), pp. 641-649

[2] T. Denk, V. Oliva and A. Materna: Mater. Sci. Forum Vol. 482 (2005), pp. 307-310

[3] A. H. Noroozi, G. Glinka and S. Lambert: Int. J. Fatigue Vol. 27 (2005), pp. 1277-1296

[4] A. H. Noroozi, G. Glinka and S. Lambert: Eng. Fract. Mech. Vol. 75 (2008), pp. 188-206

[5] K. N. Smith, P. Watson and T. H. Topper: J. Mater. Vol. 5 (1970), pp. 767-778

[6] R. C. McClung and H. Sehitoglu: Eng. Fract. Mech. Vol. 33 (1989), pp. 237-252

[7] V. Oliva, L. Cseplo, A. Materna et al.: Mater. Sci. Eng., A Vol. 234 (1997), pp. 517-520

[8] O. Partl: Research report V-KMAT-341/92 (Fac. Nuc. Sci. Phys. Engng, Czech Rep. 1992).

[9] Marc 2007r1 – Volume D (MSC.Software Corporation 2007).

[10] A. Fatemi and L. Yang: Int. J. Fatigue Vol. 20 (1998), pp. 9-34